Alterations in Physical Cross-Linking Modulate Mechanical Properties of Two-Phase Protein Polymer Networks

Xiaoyi Wu,[†,§] Rory Sallach,[§] Carolyn A. Haller,[†] Jeffrey A. Caves,[§] Karthik Nagapudi,[||] Vincent P. Conticello,[‡] Marc E. Levenston,[⊥] and Elliot L. Chaikof*[,†,§,#]

Departments of Surgery and Chemistry, Emory University, Atlanta, Georgia 30332, Department of Biomedical Engineering, Emory University School of Medicine and Georgia Institute of Technology, Atlanta, Georgia 30332, Merck & Company, Rahway, New Jersey 07095, Schools of Mechanical and Chemical Engineering, Georgia Institute of Technology, Atlanta, Georgia 30322

Received May 22, 2005; Revised Manuscript Received September 21, 2005

Physically cross-linked protein-based materials possess a number of advantages over their chemically cross-linked counterparts, including ease of processing and the ability to avoid the addition or removal of chemical reagents or unreacted intermediates. The investigations reported herein sought to examine the nature of physical cross-links within two-phase elastin−mimetic protein triblock copolymer networks through an analysis of macroscopic viscoelastic properties. Given the capacity of solution processing conditions, including solvent type and temperature to modulate the microstructure of two-phase protein polymer networks, viscoelastic properties were examined under conditions in which interphase block mixing had been either accentuated or diminished during network formation. Protein networks exhibited strikingly different properties in terms of elastic modulus, hysteresis, residual deformability, and viscosity in response to interdomain mixing. Thus, two-phase protein polymer networks exhibit tunable responses that extend the range of application of these materials to a variety of tissue engineering applications.

Introduction

The emergence of genetic engineering of synthetic polypeptides has recently enabled the preparation of multiblock protein copolymers composed of complex peptide sequences in which individual blocks may have distinct mechanical, chemical, or biological properties.[1,2] For example, Cappello and colleagues[3] have produced a series of protein polymers ranging up to 1000 amino acids in size (∼85 kDa) that contain both silk− and elastin−mimetic sequences. Silk-like regions consisting of between 12 and 48 alternating alanine and glycine residues are capable of crystallizing to form virtual cross-links between elastin−mimetic sequences composed of repeating Val-Pro-Gly-Val-Gly pentapeptides that form short blocks of between 40 and 80 amino acids. Likewise, Meyer and Chilkoti[4] have genetically engineered an elastin−mimetic protein diblock copolymer consisting of 124 pentapeptides, in which one of the two blocks was designed to phase separate under physiologic conditions. Recently, we have developed a modular convergent biosynthetic strategy that has facilitated the synthesis of high molecular weight recombinant protein block copolymers with significant flexibility in the selection and assembly of blocks of diverse size and structure.[5,6] This has led to the synthesis of a new class of BAB protein triblock copolymer that is derived from elastin−mimetic polypeptide sequences in which identical endblocks of a hydrophobic, plastic-like sequence $[(IPAVG)_4(VPAVG)]_{16}$ are separated by a central hydrophilic, elastomeric block $[(VPGVG)_4(VPGEG)]_{48}$. The triblock protein copolymer acts as a two-phase network when hydrated, in that the hydrophilic block remains conformationally flexible and elastomeric while the hydrophobic block forms virtual cross-links through thermally reversible hydrophobic aggregation. The distinct elastomeric and plastic mechanical properties of the respective blocks are analogous to those observed for many traditional synthetic thermoplastic elastomers (TPE) cast from block-selective solvents.

Akin to synthetic TPEs, the morphology and consequently the mechanical properties of the protein block copolymers can be changed by appropriate choice of solvent and film casting temperature. For example, protein triblock films cast from water above and below the hydrophobic aggregation temperature may show different levels of phase separation. When these films are rehydrated under physiologically relevant conditions, the hydrophobic microdomains are sparingly hydrated and act as virtual or physical cross-links that are much less deformable than the elastomeric matrix. However, if there are regions in which substantial mixing of both hydrophobic and hydrophilic blocks occur, the solubility and deformability behavior may be intermediate to that observed for either domain alone. Further phase-mixing of domains can be induced by casting protein films

* Address correspondence to Elliot L. Chaikof, M.D., Ph.D., 1639 Pierce Drive, Room 5105, Emory University, Atlanta, GA 30322. Phone: (404) 727-8413. Fax: (404) 727-3660. E-mail: echaiko@emory.edu.

† Department of Surgery, Emory University.

‡ Department of Chemistry, Emory University.

§ Emory University School of Medicine and Georgia Institute of Technology.

|| Merck & Company.

⊥ School of Mechanical Engineering, Georgia Institute of Technology.

School of Chemical Engineering, Georgia Institute of Technology.

10.1021/bm0503468 CCC: $30.25
Published on Web 10/19/2005

from 2,2,2-trifluoroethanol (TFE), which is a good solvent for both the blocks. Thus, stability and mechanical responses of these protein networks are inherently a function of the nature of the physical cross-link and the degree of phase separation.

The virtual cross-links formed due to hydrophobic aggregation can be deformed or even broken if the external stress is sufficiently high. Thus, the density and strength of the virtual cross-link will be an important determinant of both mechanical responses and long-term material stability. Likewise, protein chains will entangle within the solvent swollen domain, and the extent of entanglements and their capacity to break and reform dynamically in response to stress will have a profound impact on mechanical properties. As in the case of stress-induced deformation and/or disruption of virtual cross-links, breaking and reforming of chain entanglements will influence the degree to which material properties exhibit a dependence on deformation history.

Physically cross-linked protein-based materials possess a number of advantages over their chemically cross-linked counterparts, including ease of processing and the ability to avoid the addition or removal of chemical reagents or unreacted intermediates. However, to broaden their potential range of applications and develop a rational framework for the design of new materials, the relationship between mechanical behavior of protein-based thermoplastic elastomers and those nanoscale features which dictate the state of physical cross-linking must be defined under static and dynamic loading conditions over a range of time scales. Specifically, the investigations reported herein sought to examine the nature of physical cross-links within two-phase elastin−mimetic protein triblock copolymer networks through an analysis of macroscopic viscoelastic properties. Given the capacity of solution processing conditions, including solvent type and temperature, to modulate the microstructure of two-phase protein polymer networks, viscoelastic properties were examined under conditions in which interphase block mixing had been either accentuated or diminished during network formation.

Materials and Methods

Preparation of Protein Polymer Networks. A 165 kD amphiphilic protein triblock copolymer, designated **B9**, was expressed from *E. coli* and purified as detailed elsewhere.[7] The protein triblock incorporates identical endblocks of a hydrophobic sequence $[(IPAVG)_4(VPAVG)]_{16}$ separated by a central hydrophilic block $[(VPGVG)_4(VPGEG)]_{48}$. The repeat sequences were designed such that the inverse temperature transition (T_t) of the endblocks resided at or near 20 °C, while that of the central repeat unit was significantly higher than 37 °C. Amino Acid Compositional Analysis, **B9**. Calcd. (mol %): Ala, 8.1; Glx, 2.4; Gly, 31.9; Ile, 6.4; Pro, 20.0; Val, 31.2. Obsd. (mol %): Ala, 10.8; Glx, 2.0; Gly, 28.3; Ile, 7.0; Pro, 22.8; Val, 28.2. MALDI-TOF mass spectrometry, Obsd. (Calcd.): **B9**, 165 356 (165 564).

Lyophilized proteins were dissolved at a concentration of 100 mg/mL either in 2,2,2-trifluoroethanol (TFE) at 23 °C or in distilled molecular-grade water (MediaTech, Inc.) at 4 °C. The protein solution was then poured into Teflon casting molds and solvent evaporation performed either at 23 °C (TFE-23) under ambient conditions or at 4 °C (water-4) in a cold room at 50% relative humidity. After complete solvent evaporation, films were hydrated in phosphate-buffered saline (PBS) at 37 °C, which contained NaN_3 at 0.2 mg/mL to prevent biological contamination. Samples were cut into a dog-bone shape using a stainless steel die with gauge dimensions of 13 mm × 4.75 mm. Hydrated film thickness was typically 0.1 mm, as measured by optical microscopy.

Mechanical Analysis. General Methods. Mechanical characterization of protein films was performed on a dynamic mechanical thermal analyzer DMTA V (Rheometric Scientific, Inc., Newcastle, DE) with a 15 N load cell in the inverted orientation, so that samples could be immersed in a jacketed beaker filled with PBS at 37 °C. The maximum travel distance of the drive shaft of DMTA was 23 mm, which limited maximum strain to 70% of strain. Figures presented in the manuscript are representative of multiple data sets in which variability was <10%.

Uniaxial Tension. Loading and unloading was controlled by displacement at a fixed rate of 5 mm/min. Ten samples were prepared for each group of films. Three samples were monotonically stretched to about 65% of maximum strain. The remaining samples were initially stretched to specified strains and then unloaded to the zero-stress state before they were stretched to 65% strain. To simplify the loading history that may influence strain-induced damage and, as a consequence, mechanical hysteresis, each sample was subjected to one cycle of loading, unloading, and reloading. Because unloading was also controlled by displacement, and sample buckling was not desirable, unloading times were estimated for each test. Although the Young's modulus may be used to estimate unloading times, viscosity and nonlinear unloading behavior complicated this estimation. Thus, some trial and error was required to estimate ideal unloading times.

Small lags of up to 3% strain were observed in many stress−strain curves due to imperfect sample loading and were removed by curve shifting (Figure S1 in Supporting Information). Further, monotonic stress−strain curves were interpolated for samples during unloading and reloading and a mean stress calculated (Figure S2). A normalized variability, defined as the standard deviation of stress over the mean stress, was used as a measure of variability of experimental data collected from different samples (Figure S3). The mean monotonic stress−strain curve was then used as a master curve, to which all the cyclic loading curves were aligned. After curve shifting, experimental data were scattered at small strains due to imperfect sample loading with normalized variability up to 14% in TFE-23 films and 22% in water-4 films. That is, samples were not perfectly aligned to the loading direction before testing, and a real alignment of samples took place when a load was applied. Normalized variability dropped after samples were aligned to the loading direction during the first 10% strain to within 5% in TFE-23 films and 10% in water-4 films.

Stress Relaxation and Creep. Four to six samples were prepared for stress-relaxation analysis. Each sample was stretched at 5 mm/min to a given strain, and evolution of

stress over time was examined. Measurement of stress relaxation was limited to 40 min. Six to ten samples were prepared for creep analysis. Constant engineering stresses were applied for time periods up to 15 h, and the strain was monitored.

Rheology. Dynamic frequency- and time-sweep experiments were performed in tension to investigate material rheology. A constant, static stress was applied to all samples to prevent sample buckling and a 0.5% dynamic strain added. The combined static and dynamic deformation was within the linear elastic region of each sample, so that the influence of plasticity and nonlinear behavior on rheological measurements was limited. Frequency varied from 0.1 rad/s to 100 rad/s in dynamic frequency sweep and was specified in dynamic time-sweep studies. Data were collected on at least two to three replicate samples.

Results and Discussions

Conceptual Framework for Analysis of Thermoplastic Protein Triblock Copolymers. Segregation of polymer blocks into distinct domains is favored when multiblock copolymers are cast from a solvent that selectively solvates one of the component blocks. In the case of **B9**, microphase separation is favored when cast from water which preferentially solvates the hydrophilic midblock. In contrast, TFE solvates both blocks and promotes significant interpenetration of hydrophobic and hydrophilic domains.[7] Since the protein concentration of the casting solution is fivefold greater than the gelation concentration, protein chains are densely entangled. However, given differences in solvent-mediated interphase block mixing, significant differences arise in the degree of phase-mixing and the nature of the physical cross-link in TFE and water cast protein networks.

Calorimetric measurements of the triblock protein polymer confirmed that the T_t of the midblock lies well above 37 °C, while that of the hydrophobic endblocks was noted at 23 °C. Thus, it was anticipated that, upon hydration of water cast films in PBS at 37 °C, protein chains within the hydrophilic domains would be conformationally flexible, and chain entanglements would respond dynamically to an imposed force, breaking and reforming in response to stress. In contrast, these conditions were expected to induce coacervation of the hydrophobic endblocks with formation of segregated domains of semiflexible protein chains that would act as physical or virtual cross-links. From a thermodynamic standpoint, both the TFE and water cast films should show the same mechanical behavior when rehydrated in PBS. The differences that arise between the films can be ascribed to kinetics. Thus, to make meaningful interpretation of the results, the physical stability of the films when rehydrated needs to be investigated. The physical stability of both TFE and water cast films was initially confirmed by the observation that their weight and uniaxial stress−strain behavior were unchanged, despite storage in PBS at 37 °C for periods exceeding two months (data not shown). In principle, all virtual cross-links are deformable and may be broken under sufficiently high stress. Thus, the characterization of viscoelastic responses provides a useful approach for defining the deformability and strength of physical cross-links, as well as the capacity of initial casting solvent to influence virtual cross-link microstructure.

Conceptually, within the elastomeric domain of thermoplastic elastomers, chains between entanglements are flexible, and entropy-driven conformational changes of the polymer backbone are largely responsible for elasticity.[8] In contrast, within virtual cross-link sites, enthalpy-driven bending of chains occurs in response to an imposed stress.[9] The free energy F of protein chains is given as

$$F = E_{\text{int}} - TS \tag{1}$$

where S is the sum of the conformational and mixing entropy, T is the absolute temperature, and E_{int} is internal energy modulated by bending of chains. When virtual cross-links are broken under sufficiently high stress, permanent deformation or plasticity will result. Given this framework, measurements in uniaxial tension, including stress relaxation and creep, were performed to identify the maximum stress under which [$(IPAVG)_4$(VPAVG)]-based virtual cross-links maintain their mechanical integrity. Admittedly, an external stress may also produce alterations in material properties by dynamically breaking and reforming protein chain entanglements that exist *outside* of virtual cross-link sites. As such, measures of equilibrium elastic modulus and viscosity were obtained to gain insight into the density of protein chain entanglements and their response to stress.

The Instantaneous Elastic Modulus of Protein Triblock Networks Is Strongly Dependent on Film Casting Conditions. Uniaxial tensile analysis revealed an elastic modulus of 35 MPa for TFE-23 and 1.3 MPa for water-4 films (Figures 1b and 2b). For water cast films, rubber elasticity theory predicts that under equilibrium conditions the Young's modulus is inversely proportional to the average length of polymer chains between entanglements. However, since this set of experiments does not ensure equilibrium conditions, the modulus determined from uniaxial tensile analysis was referred to as an *instantaneous* elastic modulus. Indeed, equilibrium elastic moduli were obtained from studies of creep and stress relaxation, to be described below, and revealed significant nonequilibrium contributions of viscosity in uniaxial stress−strain studies.

Conditions that Promote Interdomain Mixing Lead to Significant, Though Partially Reversible, Residual Strain Deformation and Mechanical Hysteresis. Samples were stretched to various strains (10%, 20%, 30%, 40%, 50%) and then unloaded to zero stress (Figures 1a, 2a). The instantaneous residual strain was measured after sample unloading at zero stress. Water cast films exhibited small, instantaneous residual strains, typically within a few percent when unloaded from 50% strains or less (Figure 1b). In contrast, large, instantaneous residual strains were observed in TFE cast films (Figure 2b). Plastic flow occurred at an imposed stress of 1.2 MPa due to disruption of chains in TFE cast films at ~1 MPa stress.

Unexpectedly, it was noted that the instantaneous residual strains initially observed in TFE-23 films were not completely irreversible. As Ferry has noted,[10] a zero-stress state from cyclic loading does not necessarily correspond to a state

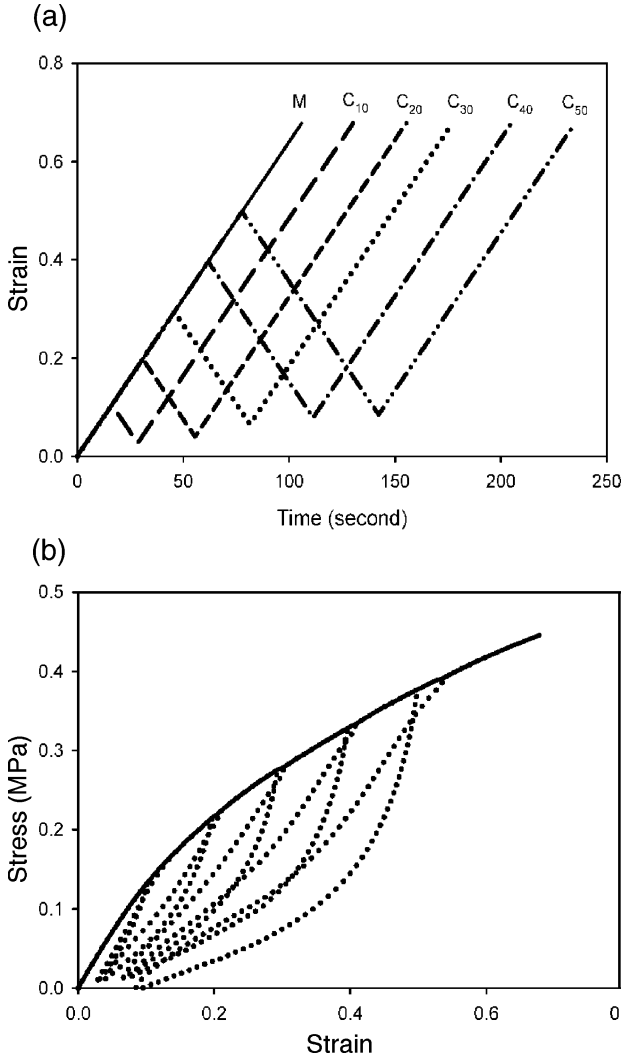

Figure 1. (a) The deformation histories of water cast films. Monotonic loading (M). Cyclic loading at 10% strain (C_{10}), at 20% strain (C_{20}), at 30% strain (C_{30}), at 40% strain (C_{40}), and at 50% strain (C_{50}). To simplify deformation history, each cyclically loaded sample was unloaded only once before it was reloaded to 65% strain. The unloading time was estimated to avoid sample buckling, as well as to achieve near-zero stress state when a sample was unloaded. (b) Uniaxial tensile stress−strain analysis of water cast films. Samples were analyzed following the loading paths specified in Figure 1a. The solid line represents an average response from eight samples and serves as a master curve, to which all the cyclic loading curves represented by dotted lines were aligned. Young's modulus measured from the first 10% strain was 1.3 MPa. Small residual strains suggest viscous−elastic characteristics of water cast films.

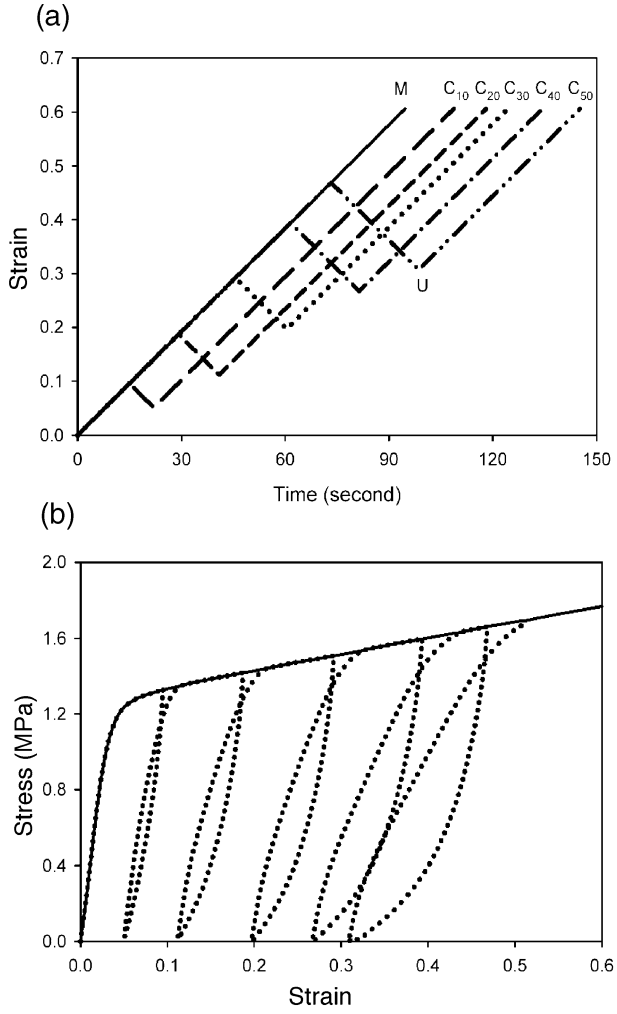

Figure 2. (a) The deformation histories of TFE cast films. Monotonic loading (M). Cyclic loading at 10% strain (C_{10}), at 20% strain (C_{20}), at 30% strain (C_{30}), at 40% strain (C_{40}), and at 50% strain (C_{50}). Each cyclically loaded sample was unloaded only once before reloading to 60% strain. The unloading time was estimated to avoid sample buckling, as well as to achieve near-zero stress state when a sample was unloaded. (b) The uniaxial tensile stress−strain analysis of TFE cast films. Samples were analyzed following the loading paths detailed in Figure 2a. The solid line represents an average response from eight samples and serves as a master curve, to which all the cyclic loading curves represented by dotted lines were aligned. Young's modulus measured from the first 5% strains was 35 MPa. TFE cast films demonstrate plastic characteristics, with yield at 1.2 MPa and large residual strain from cyclic loading.

of zero-stored energy, because some polymer chains may be stretched and others compressed to balance the tensile stress. In addition, the friction force due to the interaction between protein chains and solvent molecules may to some extent balance tensile stress in protein chains when the sample is unloaded. If deformation of the protein film is held at zero stress after unloading, the friction force that is responsible for viscosity will vanish as the motion of protein chains ceases. As a consequence, the tensile stress in some polymer chains that has not been completely relaxed will be revealed. As illustrated in Figure 3, a TFE-23 sample was stretched to 50%, unloaded to zero stress, and then held at constant deformation. Tensile stress was rapidly restored in the first tens of seconds and then gradually increased over the next 30 min until the measured stress approached 0.3 MPa. This *inverse* stress relaxation is largely due to loss of the friction force and long-range conformational rearrangements of polymer chains, which involve coordinated rearrangements of a number of entanglements. These rearrangements occur over tens of seconds or even long time periods in high molecular weight polymers.[8] All of this suggests that the instantaneous residual strain measured from unloading does not represent true plastic strain, which is permanent. Indeed, we observed that nearly half of the instantaneous residual strains measured at zero stress were recoverable after overnight incubation in PBS at 37 °C (Figure 4).

The loading−unloading loop in uniaxial stress−strain analysis is referred to as mechanical hysteresis and is a measure of energy consumption during cyclic loading. Nearly

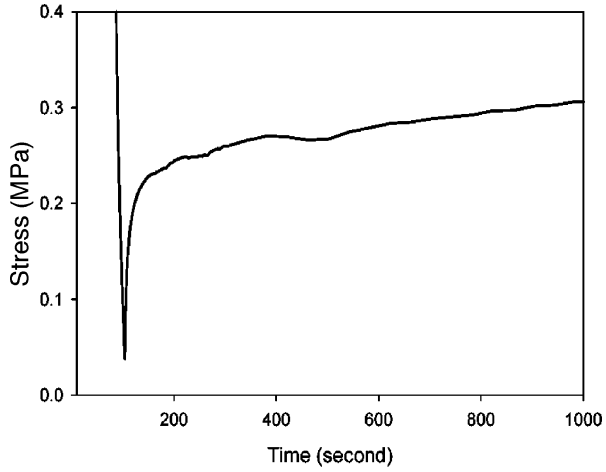

Figure 3. A representative inverse stress relaxation of TFE cast films. A TFE-23 sample was stretched to 50% strain, unloaded to nearly zero stress, as shown in Figure 2a (denoted U), and then, deformation was held constant. Tensile stress was gradually restored over 30 min (data not completely shown). Reproducibility was examined on three replicate samples.

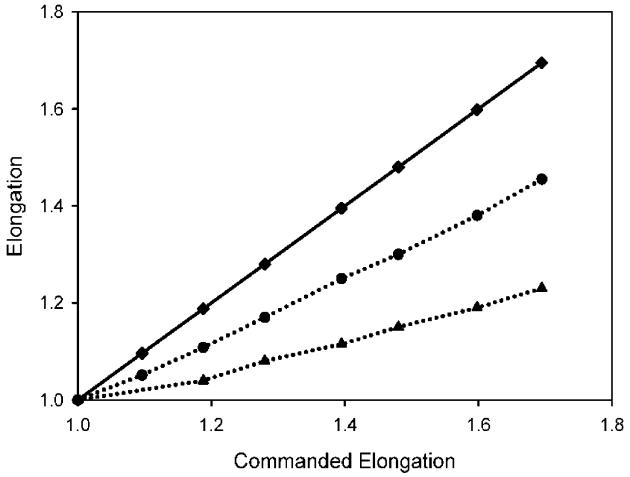

Figure 4. The recovery of the transient residual deformation of TFE cast films. Commanded elongation (◆); elongation at zero stress from unloading (●); elongation after recovery (▲). TFE cast films were stretched to commanded elongations, then were unloaded to zero stress. The gauge lengths of those deformed samples were measured after being recovered in PBS at 37 °C overnight. This recovery study suggests that the transient residual strain measured at zero stress from cyclic loading is partially recoverable.

complete energy recovery would be associated with minimal hysteresis. Significantly, the observation of *inverse* stress relaxation suggests that the hysteresis loop does not provide an accurate measure of energy loss for TFE-23, because stored energy is not completely released at zero stress. In contrast, *inverse* stress relaxation was not expected be a relevant event for water cast films, since these materials displayed small instantaneous residual strains.

Deformation-Induced Plastic Flow Occurs Due to Differential Disruption of Virtual Cross-links and/or Chain Entanglements. Deformation-induced material softening observed after the initial loading cycle was noted for both TFE and water cast samples and is related to strain-induced damage.[11] Small residual strain in water-4 films suggests that virtual cross-links remain largely intact (Figure 1a). Thus, strain-induced softening in water-4 films is likely attributable to rearrangements and/or loss of chain entanglements in the hydrophilic solvent swollen midblock. However, in TFE-23 films, disruption of chains at deformations that exceed 10% strain is probably responsible for observed plastic flow. To distinguish strain-induced damage from a viscous response, TFE-23 samples initially stretched to 65% strain through different loading paths were allowed to recover for one week in PBS at 37 °C after which uniaxial tensile testing was repeated. The Young's modulus and yield stress of the recovered sample were 25 MPa and 0.9 MPa, respectively, which reveals some degree of strain-induced damage due to a modest reduction of these parameters when compared to those measured at the time of initial film testing (Young's modulus 35 MPa, yield stress 1.2 MPa).

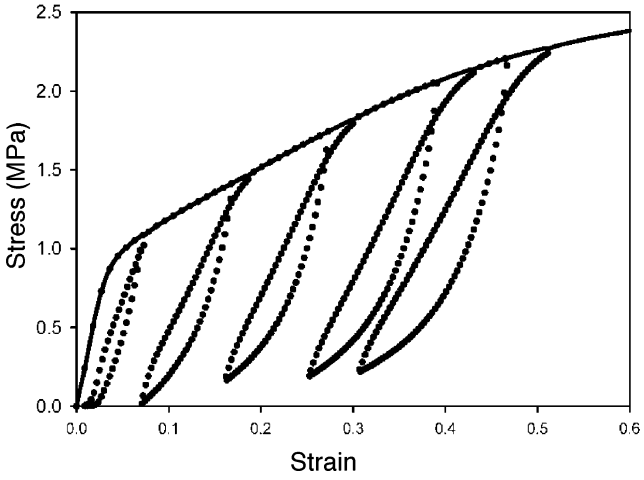

Figure 5. Uniaxial tensile analysis of recovered TFE cast films. TFE cast films were stretched to 60% following different loading paths as shown in Figure 2a. The deformed films were recovered in PBS at 37 °C for one week, and then subjected to uniaxial tensile analysis. Young's modulus was measured at 25 MPa, and yield point at 0.9 MPa. A reduction in Young's modulus and yield points suggest an effect of strain-induced damage in TFE cast films.

Stress Relaxation and Creep Data Reveal Equilibrium Elastic Moduli that Are Significantly Lower than Those Determined from Uniaxial Stress−Strain Analysis. When deformation is held constant, a relaxation of imposed tensile stresses may be observed due to vanishing friction forces, conformational rearrangement of polymer chains, and strain-induced damage. In both film types, a rapid relaxation of stress was observed in the first tens of seconds with a stabilization of relaxed stress after 30 min that provides a time scale for conformational rearrangements of protein chains and network entanglements. Water-4 films exhibited a 40% decrease in engineering stress from 0.45 to 0.26 MPa at 70% strain, while stress relaxation for TFE-23 films approached 70% at 60% strain (Figures 6and 7). All of this is consistent with previously measured differences in hysteresis.

Once stress relaxation reaches a steady state, an equilibrium elastic modulus may be calculated by following nonlinear elasticity theory[12]

$$\sigma = E/3(\lambda - 1/\lambda^2) \qquad (2)$$

where σ is engineering stress, E is tensile elastic modulus, and λ is elongation. At small strains, eq 2 reduces to linear elasticity $\sigma = E{\cdot}\Delta\lambda$, where $\Delta\lambda$ is the increment of elongation

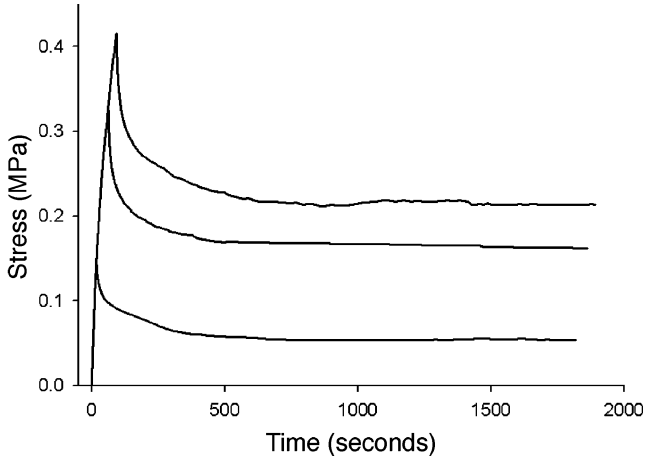

Figure 6. Stress relaxation of water cast films. Water cast samples were stretched to 10%, 40%, and 60% strains at constant rate of 5 mm per minute, and stress relaxation was then recorded over time as deformation was held constant.

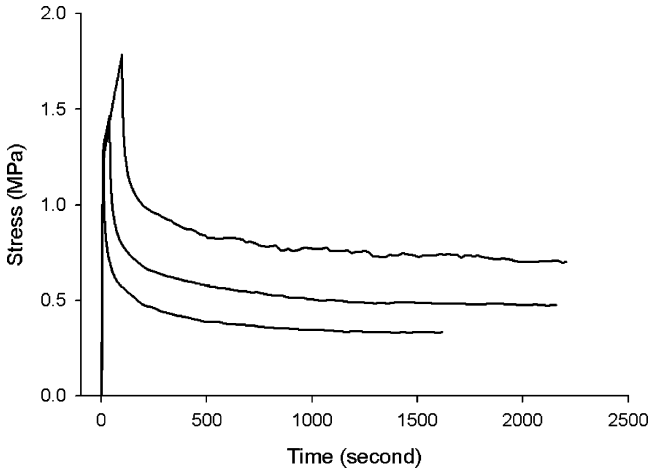

Figure 7. Stress relaxation of TFE cast films. TFE cast samples were stretched to 5%, 25%, and 60% strains and stress relaxation examined.

or strain. The equilibrium elastic modulus for water cast films is 0.6 MPa calculated at 70% strain and is lower than the instantaneous modulus (1.3 MPa) measured at 10% strain. When the deformation time is not sufficient for chains to rearrange their conformations, as in the case of the instantaneous elastic modulus, materials tend to be stiffer. However, at large deformations, strain-induced damage may lower the equilibrium elastic modulus.

Creep behavior of water cast and TFE cast samples are shown in Figures 8 and 9. As expected, the creep of the water cast samples was found to be higher than the creep of TFE cast samples at similar stress levels (0.2 MPa). If creep strain reaches equilibrium strain ϵ_e under an applied stress σ, the equilibrium compliance J_e can be obtained

$$J_e = \epsilon_e/\sigma \tag{3}$$

In turn, the reciprocal of the equilibrium compliance is the equilibrium elastic modulus. Using this approach, calculated equilibrium elastic moduli for water-4 films ranged from 0.9 to 1.4 MPa for stress levels between 0.2 and 0.25 MPa and were comparable to the equilibrium elastic modulus of 0.6 MPa measured from stress relaxation at 70% strain (Figure

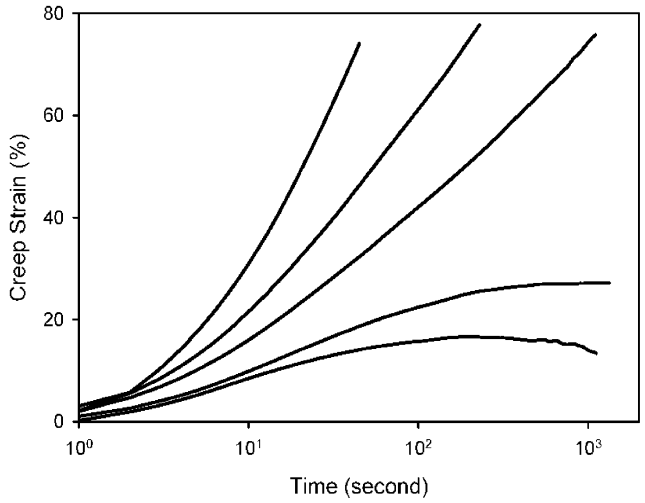

Figure 8. Creep of water cast films. From left to right, creep was examined as tensile stresses were maintained at 0.5, 0.4, 0.3, 0.25, and 0.2 MPa, respectively. Creep was locked when stress was lower than 0.25 MPa.

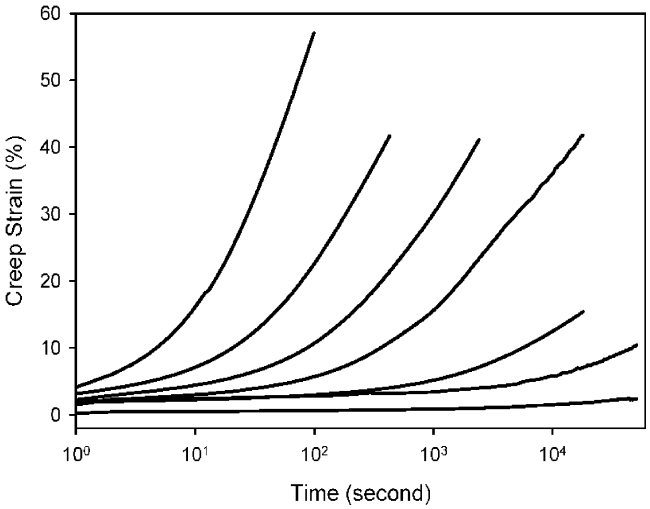

Figure 9. Creep of TFE cast films. From left to right, creep was examined as tensile stress was maintained at 1.4, 1.2, 1.0, 0.8, 0.6, 0.4, and 0.2 MPa, respectively. Creep was locked when stress was lower than 0.2 MPa.

8). Of note, the equilibrium elastic modulus measured from creep under 0.2 MPa stress was close to the instantaneous elastic modulus determined from uniaxial stress−strain analysis, which suggests that deformation at constant rate of 5 mm/min was near equilibrium at small strains. Similarly, under an applied stress of 0.2 MPa, creep strain approached 2.3% in TFE-23 films and was associated with a calculated equilibrium elastic modulus of 9 MPa, consistent with stress-relaxation data at 5% deformation (7 MPa). However, in this instance, the equilibrium elastic modulus was much lower than the instantaneous modulus (35 MPa) and provides additional confirmation that equilibrium was not achieved under the conditions of uniaxial stress−strain studies. In other words, the strain rate was not sufficiently slow for protein chains to complete conformational rearrangements. All told, the stress relaxation and creep data highlight that mechanical property analysis derived solely from uniaxial stress−strain studies may not necessarily reflect equilibrium values and should be used with some degree of caution.

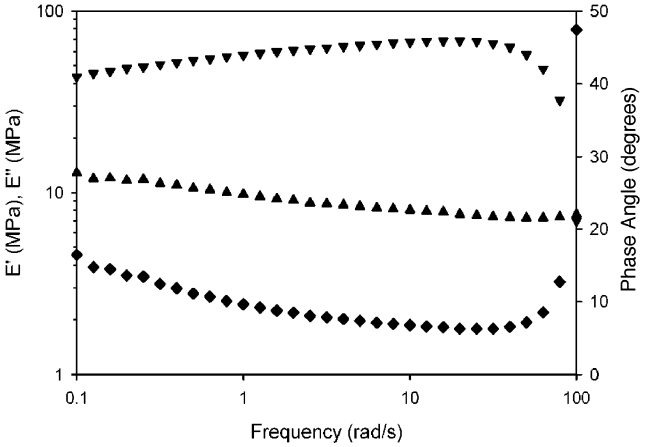

Figure 10. Frequency sweep spectra of TFE cast film in the tension mode. Storage modulus E' (▼); loss modulus E'' (▲); and phase angle (δ) (◆). A constant static force of 30 g was maintained throughout experiment to prevent sample buckling. Then, 0.5% dynamic strain was added to obtain the frequency sweep spectra. A dramatic increase in phase angle at 100 rad/s indicates dynamic bulking of samples. Reproducibility of experiments was examined on three replicate samples.

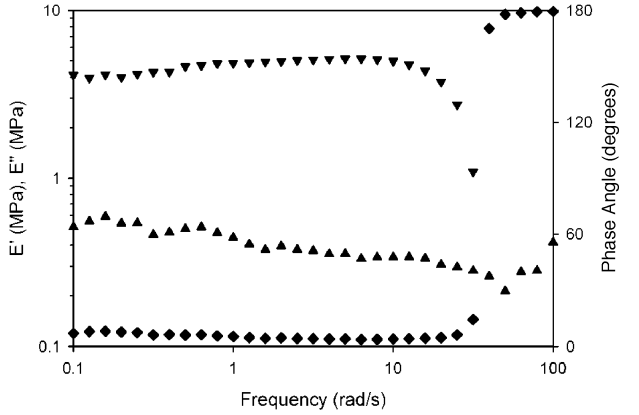

Figure 11. Frequency sweep spectra of water cast film in tension mode. Storage modulus E' (▼); loss modulus E'' (▲); and phase angle (δ) (◆). Dynamic strain of 0.5% was added to a baseline static force of 10 g, which was maintained throughout testing to prevent sample from buckling. The storage modulus decreased at frequency above 20 rad/s and became negative at 60 rad/s as indicated by a phase angle of 180°, which was due to dynamic buckling of samples. Reproducibility of experiments was examined on three replicate samples.

The degree of chain entanglements in water cast films suggest participation of both the midblock and the end block in the mechanical response.

In uniaxial tension, the tensile force f can be obtained from

$$f = \frac{\partial E_{\text{int}}}{\partial L} - T\frac{\partial S}{\partial L} \tag{4}$$

where L is the current length of a sample and $\delta E_{\text{int}}/\delta L$ denotes the contribution of enthalpy to deformation. If the contribution of enthalpy can be neglected, the elastic modulus provides a measure of the average molecular weight between two adjacent entanglement sites[8,13]

$$\mathrm{E} = \frac{3\rho \mathrm{RT}}{\mathrm{M_c}} \tag{5}$$

where ρ is the density, R is the molar gas constant, T is the absolute temperature, and M_c is the molecular weight between entanglements. The equilibrium elastic modulus was 1.3 MPa for water-4 films at a *protein* concentrations of 0.6 g/cm^3. Thus, the average molecular weight between chain entanglements was calculated to be 3600 mu for water-4 films. As the average molecular weight of an amino acid is ~100 mu, these results suggest that, when cast from water as a selective solvent that favors endblock segregation, cross-links are separated by 30−40 amino acids. While this suggests that conformational changes of flexible midblock chains could account for at least a portion of the deformation in water-4 films, this cross-link separation is much smaller than the size of the midblock and implies that the contribution of semiflexible endblock chains should not be excluded. This notion was further supported by rheological analysis.

Rheological Behavior Is Consistent with the Effects of Hydrophobic Hydration on Protein Network Elasticity. The storage (E') and loss (E'') moduli were examined through a frequency sweep between 0.1 rad/s and 100 rad/s. Figures 10 and 11 demonstrate that the loss modulus decreased slightly with increasing frequency, while the storage modulus increased until a decrease was noted at high frequency. At high frequencies, the time during each period of deformation decreases, which limits polymer chain rearrangement so that materials tend to stiffen, and consequently, the storage modulus often increases. Sample buckling that was prevented at lower frequencies occurred and resulted in a decrease in storage modulus at high frequencies. Elastic modulus from unloading was typically higher than that from uploading (Figures 1b and 2b), and their differences became sufficiently larger at higher frequencies, resulting in dynamic buckling.

Prior to dynamic buckling at high frequencies, values for the loss tangent, tan δ (E''/E'), were consistent with mechanical hysteresis responses. Tan δ values were 0.24 and 0.12 for TFE and water cast films, respectively, suggesting greater energy loss in TFE cast samples. When frequencies were fixed at 10 rad/s for TFE-23 and 1 rad/s for water-4 films, the storage and loss moduli did not change appreciably over time and suggested that at small strains polymer chains do not reorient along the loading direction (Figure 12).

Conclusions

The viscoelastic properties of protein networks prepared under different casting conditions from an identical elastin-derived protein copolymer were characterized by uniaxial tensile analysis, stress relaxation, creep, and rheology in tension mode. Protein networks exhibited strikingly different properties in terms of elastic modulus, hysteresis, residual deformability, and viscosity. Water cast films possessed a Young's modulus of 1.3 MPa, small residual deformation in cyclic loading, and relatively small hysteresis. At medium or large strains, deformations modified the network of chain entanglements and lead to stress softening. In contrast, TFE cast films displayed viscoplasticity, evidenced by large hysteresis and residual strains on cyclic loading. Plasticity was likely due to disruption and slippage of protein chains. Rheology in tension mode confirmed that viscous losses were higher in TFE than water cast films, which was consistent

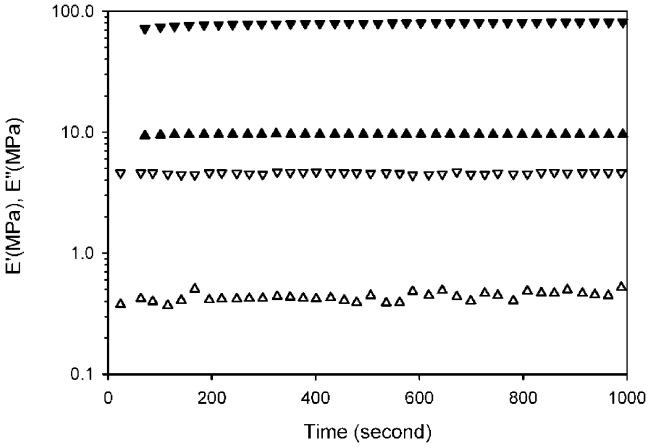

Figure 12. Time sweep spectra of TFE and water cast films. Storage modulus E' of TFE cast film (▼); loss modulus of TFE cast film E'' (▲); storage modulus E' of water cast film (▽); loss modulus of water cast film (△). On TFE cast films, 0.5% dynamic strain was added to a baseline static force of 20 g, as frequency was fixed at 5 rad/s. On water cast films, 0.5% dynamic strain was added to a baseline static force of 10 g, as frequency was fixed at 1 rad/s. Reproducibility of experiments was examined on three replicate samples.

with a higher level of mechanical hysteresis for these films. These property differences can be attributed to the effect of solvent casting conditions on interdomain mixing. Thus, appropriate choice of solvent can modulate mechanical response of protein triblock copolymers. This in turns extends the range of application of these materials to a variety of tissue engineering applications.

Acknowledgment. This work was supported by grants from the NIH.

Supporting Information Available. Figures illustrating experimental data processing and the normalized variation between samples. This material is available free of charge via the Internet at http://pubs.acs.org.

References and Notes

(1) Ferrari, F.; Cappello, J. In *Protein-Based Materials*; Kaplan, D. L., Ed.; Birkhäuser: Boston, 1997.
(2) Petka, W. A.; Harden, J. L.; McGrath, K. P.; Wirtz, D.; Tirrell, D. A. *Science* **1998**, *281*, 389−392.
(3) Cappello, J.; Crissman, J. W.; Crissman, M.; Ferrari, F. A.; Textor, G.; Wallis, O.; Whitledge, J. R.; Zhou, X.; Burman, D.; Aukerman, L.; Stedronsky, E. R. *J. Controlled Release* **1998**, *53*, 105−117.
(4) Meyer, D. E.; Chilkoti, A. *Biomacromolecules* **2002**, *3*, 357−367.
(5) Wright, E. R.; Conticello, V. P. *Adv. Drug Delivery Rev.* **2002**, *54*, 1057−1073.
(6) Wright, E. R.; McMillan, R. A.; Cooper, A.; Apkarian, R. P.; Conticello, V. P. *Adv. Funct. Mater.* **2002**, *12*, 149−154.
(7) Nagapudi, K.; Brinkman, W. T.; Leisen, J.; Thomas, B. S.; Wright, E. R.; Haller, C.; Wu, X.; Apkarian, R. P.; Conticello, V. P.; Chaikof, E. L. *Macromolecules* **2005**, *38*, in press.
(8) Gennes, P.-G. d. *Scaling concepts in polymer physics*; Cornell University Press: Ithaca, NY, 1979.
(9) Tseng, Y.; Wirtz, D. *Biophys. J.* **2001**, *81* (3), 1643−1656.
(10) Ferry, J. *Viscoelastic properties of polymers*; Wiley: New York, 1961.
(11) Marckmann, G.; Verron, E.; Gornet, L.; Chagnon, G.; Charrier, P.; Fort, P. *J. Mech. Phys. Solids* **2002**, *50*, 2011−2028.
(12) Treloar, L. R. G. *The physics of rubber elasticity*, 3rd ed.; Clarendon Press: Oxford, 1975.
(13) Flory, P. J. *Principles of Polymer Chemistry*; Cornell University Press: Ithaca, NY, 1953.

BM0503468